



香港城市大學
City University of Hong Kong

專業 創新 胸懷全球
Professional · Creative
For The World

CityU Scholars

Dopant-Free Crossconjugated Hole-Transporting Polymers for Highly Efficient Perovskite Solar Cells

Sun, Xianglang; Deng, Xiang; Li, Zhen; Xiong, Bijin; Zhong, Cheng; Zhu, Zonglong; Li, Zhong'an; Jen, Alex K.-Y.

Published in:
Advanced Science

Published: 01/07/2020

Document Version:
Final Published version, also known as Publisher's PDF, Publisher's Final version or Version of Record

License:
CC BY

Publication record in CityU Scholars:
[Go to record](#)

Published version (DOI):
[10.1002/adv.201903331](https://doi.org/10.1002/adv.201903331)

Publication details:
Sun, X., Deng, X., Li, Z., Xiong, B., Zhong, C., Zhu, Z., Li, Z., & Jen, A. K.-Y. (2020). Dopant-Free Crossconjugated Hole-Transporting Polymers for Highly Efficient Perovskite Solar Cells. *Advanced Science*, 7(13), [1903331]. <https://doi.org/10.1002/adv.201903331>

Citing this paper

Please note that where the full-text provided on CityU Scholars is the Post-print version (also known as Accepted Author Manuscript, Peer-reviewed or Author Final version), it may differ from the Final Published version. When citing, ensure that you check and use the publisher's definitive version for pagination and other details.

General rights

Copyright for the publications made accessible via the CityU Scholars portal is retained by the author(s) and/or other copyright owners and it is a condition of accessing these publications that users recognise and abide by the legal requirements associated with these rights. Users may not further distribute the material or use it for any profit-making activity or commercial gain.

Publisher permission

Permission for previously published items are in accordance with publisher's copyright policies sourced from the SHERPA RoMEO database. Links to full text versions (either Published or Post-print) are only available if corresponding publishers allow open access.

Take down policy

Contact lbscholars@cityu.edu.hk if you believe that this document breaches copyright and provide us with details. We will remove access to the work immediately and investigate your claim.

Dopant-Free Crossconjugated Hole-Transporting Polymers for Highly Efficient Perovskite Solar Cells

Xianglang Sun, Xiang Deng, Zhen Li, Bijin Xiong, Cheng Zhong, Zonglong Zhu,* Zhong'an Li,* and Alex K.-Y. Jen*

Currently, there are only very few dopant-free polymer hole-transporting materials (HTMs) that can enable perovskite solar cells (PVSCs) to demonstrate a high power conversion efficiency (PCE) of greater than 20%. To address this need, a simple and efficient way is developed to synthesize novel crossconjugated polymers as high performance dopant-free HTMs to endow PVSCs with a high PCE of 21.3%, which is among the highest values reported for single-junction inverted PVSCs. More importantly, rational understanding of the reasons why two isomeric polymer HTMs (PPE1 and PPE2) with almost identical photophysical properties, hole-transporting ability, and surface wettability deliver so distinctly different device performance under similar device fabrication conditions is manifested. PPE2 is found to improve the quality of perovskite films cast on top with larger grain sizes and more oriented crystallization. These results help unveil the new HTM design rules to influence the perovskite growth/crystallization for improving the performance of inverted PVSCs.

1. Introduction

In the past decade, the power conversion efficiency (PCE) of organic–inorganic hybrid perovskite solar cells (PVSCs) has increased rapidly from 3.8%^[1] to the certified 25.2%,^[2] showing very promising prospect as a new photovoltaic technology.^[3–6] There are three commonly used device architectures for fabricating PVSCs,^[7–9] i.e., mesoscopic nanostructures, and conventional n–i–p and inverted p–i–n planar junction structures. Among these, inverted PVSCs have certain advantages such as suppressed photocurrent-hysteresis and processing compatibility with flexible devices.^[10–13] The first report of inverted PVSC was reported by Guo and co-workers in 2013,^[14] affording a poor PCE of 3.9%. Subsequently, the PCEs of inverted PVSCs have been significantly improved to exceed

20% by applying new film-deposition methods, optimizing device configurations, and proper interfacial engineering.^[15–19]

For inverted p–i–n devices, a hole-transporting layer (HTL) is deposited first, followed by a photoactive perovskite layer, and then an electron-transporting layer (ETL). Thus, in this device architecture, HTL not only is responsible for transporting/extracting holes, but also plays an important role in affecting the growth of perovskite layer.^[20–24] Therefore, significant efforts have been devoted to regulating the surface properties of HTLs in inverted PVSCs to promote the formation of high quality perovskite films.^[22,24–28] For example, Liao and co-workers have introduced a perylene-based interlayer between the perovskite layer and poly(3,4-ethylenedioxythiophene)–polystyrenesulfonate (PEDOT:PSS) HTL to facilitate perovskite growth with enhanced crystallinity.^[27]


To date, PEDOT:PSS and poly(bis(4-phenyl)(2,4,6-trimethylphenyl)amine) (PTAA) are the two most frequently used HTMs for inverted PVSCs.^[11,12] PEDOT:PSS exhibits both a high hole conductivity due to its self-doping ability and excellent wettability with perovskite precursor solutions. However, its inherent acidic and hygroscopic characteristics have been proven to hamper the long-term stability of derived PVSCs, while the hydrophilic surface reduces the grain boundary mobility to limit grain sizes.^[29,30] In addition, large potential loss is often found for the PEDOT:PSS-based PVSCs due to mismatched work function between PEDOT:PSS and perovskites, which significantly limits their PCEs.^[11,31]

Dr. X. Sun, Prof. B. Xiong, Prof. Z. Li
Key Laboratory for Material Chemistry of Energy Conversion and Storage
Ministry of Education
School of Chemistry and Chemical Engineering
Huazhong University of Science and Technology
Wuhan 430074, P. R. China
E-mail: lizha@hust.edu.cn

X. Deng, Z. Li, Prof. Z. Zhu, Prof. A. K.-Y. Jen
Department of Chemistry
City University of Hong Kong
Kowloon, 999077 Hong Kong SAR
E-mail: zonglzhu@cityu.edu.hk; alexjen@cityu.edu.hk

X. Deng, Prof. A. K.-Y. Jen
Department of Materials Science and Engineering
City University of Hong Kong
Kowloon, 999077 Hong Kong

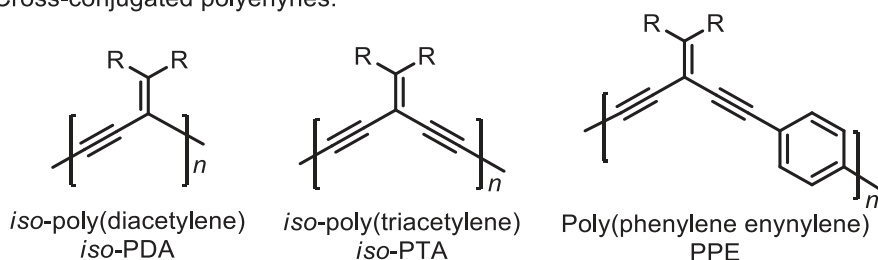
Prof. C. Zhong
Department of Chemistry
Wuhan University
Wuhan 430072 P. R. China

 The ORCID identification number(s) for the author(s) of this article can be found under <https://doi.org/10.1002/advs.201903331>

© 2020 The Authors. Advanced Science published by Wiley-VCH Verlag GmbH & Co. KGaA. This is an open access article under the terms of the Creative Commons Attribution License, which permits use, distribution and reproduction in any medium, provided the original work is properly cited.

DOI: 10.1002/advs.201903331

a: Cross-conjugated polyenyne:



b: PPEs synthesized this work:

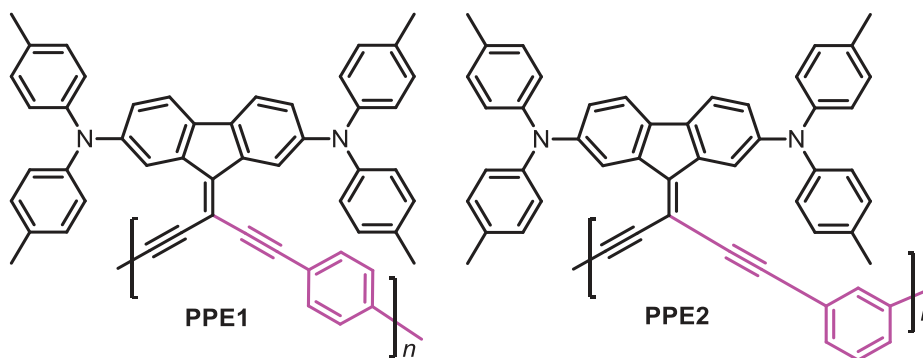


Figure 1. Structures of representative a) crossconjugated polyenyne and b) our designed **PPE1** and **PPE2** in this work.

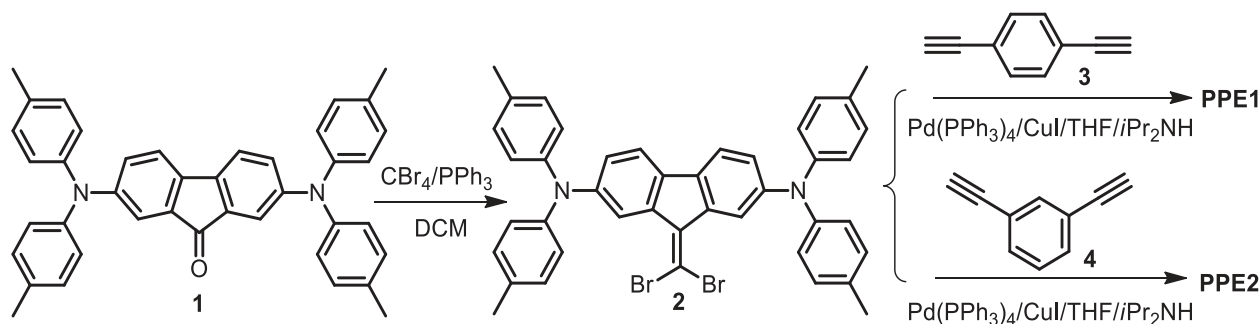
On the contrary, PTAA can produce much higher PCEs over 20%,^[17–19,32] however, it is not only quite expensive, but also requires extra chemical doping procedures to achieve high performance.^[17,24,32–34] Unfortunately, chemical doping tends to degrade device performance because of the associated oxidation reactions.^[35–38] Besides, its hydrophobic feature also increases the difficulty in coating perovskite films on top, especially for the roll-to-roll printing process.^[39] Thus, it is necessary to prewet the PTAA layer with solvent or apply an amphiphilic interlayer to facilitate the deposition of perovskites.^[18,19] Hence, it is imperative to develop new high-performance dopant-free polymer HTMs with simple synthetic procedures and suitable surface wettability for inverted PVSCs,^[26,35–38,40–43] however the progress has been quite tardy with only very few dopant-free polymer HTMs can afford PCE higher than 20% (Chart S1 and Table S1, Supporting Information).

Crossconjugated polymers have been demonstrated as an important class of organic semiconductors, due to their facile synthesis and interesting structural, physical, and optoelectronic properties.^[44–49] Among them, particular interests have been paid on developing crossconjugated polyenyne, such as *iso*-poly(diacetylene) (*iso*-PDA) and *iso*-poly(triacetylene) (*iso*-PTA) (Figure 1a), possessing efficient π -electron delocalization along the crossconjugated framework, although the extent is reduced compared to that of fully conjugated analogues.^[44,50–52] Another attracting feature for crossconjugated polyenyne is its optical transparency in the visible region even with a relatively large π -conjugation.^[53,54] This is advantageous because it can help absorb damaging UV light and avoid competing with the perovskite light absorption.¹⁹ With the abovementioned characteristics, it is worth to explore crossconjugated polymer HTMs for their applications for PVSCs.

Herein, we report the facile synthesis of *iso*-PTA derivatives as dopant-free HTMs for highly efficient inverted PVSCs. In our design, a phenyl spacer is introduced onto the *iso*-PTA backbone to form poly(phenylene enynylene)s (PPEs, Figure 1b), and by changing the linkage positions of phenyl spacers from para to meta, the backbone structure can be modified subtly to alter the crystallinity and optoelectronic properties of the resulting PPEs for investigating their influence on the perovskite properties and device performance. We further functionalize the vinylidene groups of PPEs by attaching 2,7-diphenylamine capped fluorene units, one of the basic frameworks of dopant-free HTMs,^[55–58] to improve the hole mobility. Both PPEs possess proper energy levels, moderate hole mobilities, good surface wettability to the precursor solution of perovskites, and transparent window in the visible absorption region. Surprisingly, when they were used as dopant-free HTMs for inverted PVSCs, the devices showed dramatically different PCEs, 11.13% for **PPE1** while 19.33% for **PPE2**, respectively, attributed to improved perovskite quality derived from **PPE2**. Furthermore, by rational surface passivation, the open circuit voltage (V_{oc}) of **PPE2**-based inverted PVSCs can be effectively improved to afford an impressive PCE of 21.3%.

2. Results and Discussion

The synthetic route for preparing PPEs is shown in Scheme 1, which is quite straightforward comparing with those reported for donor–acceptor type polymer HTMs.^[59–66] The synthetic details and characterization data are provided in Supporting Information. Compound **1** was synthesized from the reaction of two commercial raw materials according to our previous work,^[67] which can then be easily transferred to compound **2** via a



Scheme 1. Synthetic route of crossconjugated polyenynes PPE1 and PPE2.

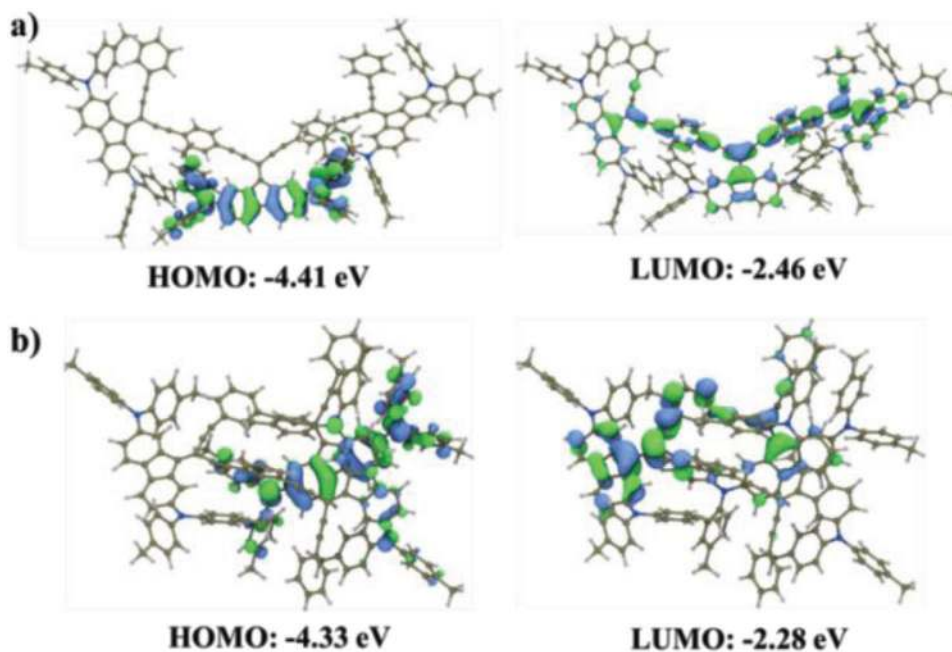


Figure 2. The DFT-optimized molecular frontier orbitals of a) PPE1 and b) PPE2 based on the analogous trimer model.

Corey–Fuchs reaction at a good yield of 71%.^[68] The designed polymers PPE1 and PPE2 were obtained from compound 2 through a typical palladium-catalyzed Sonogashira copolymerization with 1,4-diethynylbenzene (3) and 1,3-diethynylbenzene (4) to study the effect of para- and meta- conjugation on the final material properties. The copolymerized PPE1 showed a much lower yield than that of PPE2 (31.6% vs 86.1%), due to the formation of macrocycles by-products. As a result, a much higher synthetic cost of \$65.5 g⁻¹ is calculated for PPE1, while that of PPE2 is only \$20.5 g⁻¹ based on the research scale starting materials, which are much lower than that for PTAA.

The density functional theory (DFT)-optimized structures are illustrated in Figure S1 (Supporting Information) based on the analogous trimer model, while the calculated highest occupied molecular orbital (HOMO) and lowest unoccupied molecular orbital (LUMO) energy levels are shown in Figure 2. As shown, PPE1 with paraconjugation shows a linear π -conjugation but a high tendency to form macrocycles, thereby explaining its low copolymerization yield. On the contrast, PPE2 with metaconjugation exhibits an unusual Zigzag polymer structure like typi-

cal polyenynes, containing a folded conformation with closer intramolecular stacking between the diphenylamine-capped fluorene units. The torsional angles between two phenylacetylene groups and the central fluorene unit are also found to be quite different. For PPE1, it is similar with an angle of $\approx 45^\circ$, while for PPE2, there are two angles, 27° and 68° , which could be the main reason for forming folded conformation. Both PPEs showed that the electron wave of their HOMOs are localizing on the diphenylamine-capped fluorene units, while those of the LUMOs are delocalizing over the polymer backbone and partially extending to the fluorene units. The higher HOMO level for PPE2 could be due to the strong intramolecular stacking between diphenylamine moieties, while the lower LUMO level for PPE1 is possibly due to the para-type linkage enables π -conjugation to be more efficient.

Both PPEs have good solubility in organic solvents such as tetrahydrofuran (THF), chloroform (CF), chlorobenzene (CB), however, they can resist the erosion of *N,N*-dimethylformamide (DMF) and dimethyl sulfoxide (DMSO), indicating the feasibility of processing perovskite precursor solutions on top of these films. The molecular weights of these two polymers were

Table 1. Molecular weights, thermal, optical, electrochemical, and charge transfer properties of **PPE1** and **PPE2**.

HTM	M_n [g mol ⁻¹]	\bar{D}	λ_{max} ^{a)} [nm]		$E_{g,\text{opt}}$ ^{b)} [eV]	E_{HOMO} ^{c)} [eV]	E_{LUMO} ^{d)} [eV]	E_{HOMO} ^{e)} [eV]	T_d ^{f)} [°C]	Mobility ^{g)} [cm ² V ⁻¹ s ⁻¹]
			Solution	Film						
PPE1	10800	1.32	306, 384	383	2.45	-5.08	-2.63	-5.11	460	2.2×10^{-6}
PPE2	11900	1.32	310, 385	384	2.70	-5.06	-2.36	-5.08	414	1.9×10^{-6}

^{a)}Absorption maxima; ^{b)}Optical bandgaps calculated from film absorption edges; ^{c)}Measured from electrochemistry experiments; ^{d)}Calculated by subtracting $E_{g,\text{opt}}$ from HOMO levels; ^{e)}Measured from UPS experiments; ^{f)}The 5% weight loss temperature detected by TGA under nitrogen; ^{g)}Hole mobilities measured by SCLC method.

determined by gel permeation chromatography (GPC) using THF as the eluent, and the number-average molecular weight (M_n) of **PPE1** and **PPE2** were determined to be 10 800 and 11 900 g mol⁻¹, respectively, with a similar polydispersity index (\bar{D}) of 1.32, as listed in **Table 1**. The onset thermal decomposition temperatures (T_d , 5% weight loss) were measured to be 460 and 414 °C for **PPE1** and **PPE2**, respectively, based on the thermogravimetric analysis (TGA, Figure S2, Supporting Information), suggesting they possess high thermal stability. Nevertheless, no clear glass transition temperatures and melting points could be observed in the differential scanning calorimetry (DSC, Figure S3, Supporting Information) for both PPEs.

Both polymers have evident π - π^* transition band at ≈ 385 nm, accompanied with a weak intramolecular charge transfer (ICT) band due to the electron-deficient character of diacetylenephenyl groups (Figure S4, Supporting Information and Table 1). However, the ICT absorption band of **PPE1** is more red-shifted than

PPE2, owing to the more efficient paraconjugation. Moreover, it is worth to note that the absorption peak of PPEs at ≈ 320 nm, ascribed to the localized excitonic π - π^* transition of diphenylamine units, disappeared from the solution state to the film state, which could be attributed to the enhanced intermolecular interactions.

Both PPEs also exhibit good film-forming ability, and the resulting films (≈ 10 nm thick, Figure S5, Supporting Information) on indium tin oxide (ITO) substrates show uniform and smooth morphology with similar root-mean-square surface roughnesses (RMS) of 2.7 nm for **PPE1** and 2.5 nm for **PPE2**, respectively. For inverted PVSCs, good optical transparency of HTM is highly desirable because it can help absorb damaging UV light and avoid competing with the perovskite light absorption.^[41,69,70] In this regard, the transmission spectra of both polymer films on ITO are shown in **Figure 3a**, where both PPEs show similar transparency in the visible region.

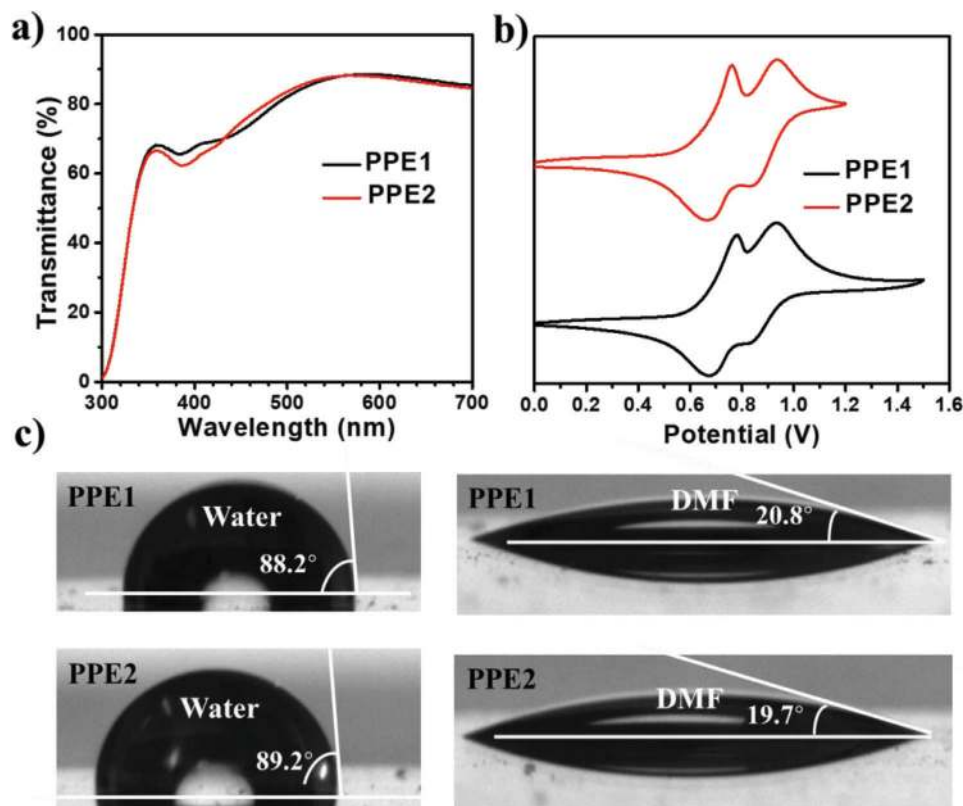


Figure 3. a) The film transmission spectra of polymer films on the ITO substrates. b) The CV curves of polymer films versus Fc/Fc^+ (0.45 V) measured in CH_3CN solutions. c) Contact angles of polymer films with respect to water and DMF drop.

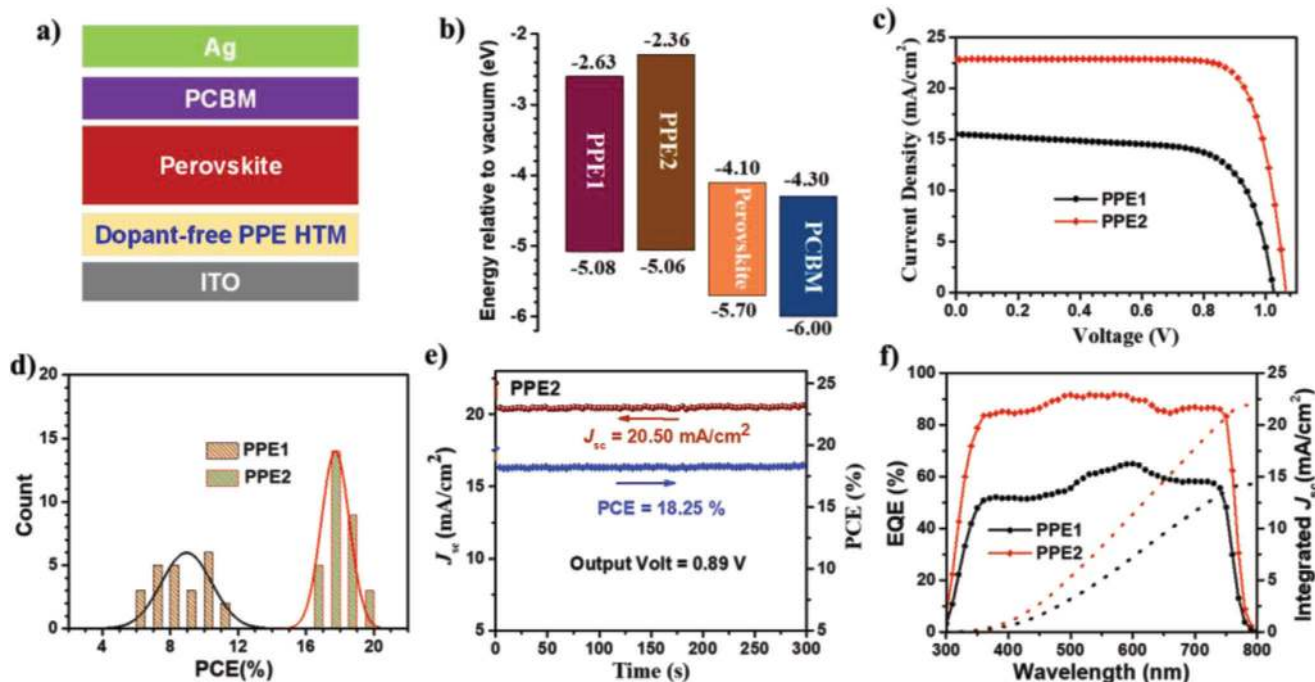


Figure 4. a) Device structure used in this study; b) corresponding energy levels relative to perovskite and PCBM; c) J - V curves of the champion PVSCs with PPEs as dopant-free HTMs; d) Histograms of efficiency distributions of fabricated PVSCs; e) stable output current of PPE2-based inverted PVSC under a constant bias of 0.89 V; f) EQE spectra with the integrated short-circuit current density for champion PVSCs.

The cyclic voltammetry (CV) curves of polymer films are shown in Figure 3b, with the related data listed in Table 1. The first average oxidation potentials (E_{ox}) of PPE1 and PPE2 versus Fc/Fc^+ (0.45 eV) were found to be 0.28 and 0.26 V, respectively, corresponding to the HOMO levels of -5.08 and -5.06 eV based on an equation of $E_{\text{HOMO}} = -(E_{\text{ox}} + 4.80)$ eV. Moreover, the optical bandgaps ($E_{\text{g,opt}}$ s) of PPE1 and PPE2 films are calculated to be 2.45 and 2.70 eV, respectively, based on the film absorption onsets. By subtracting $E_{\text{g,opt}}$ s from the HOMO levels, the LUMO energy levels of PPE1 and PPE2 are estimated as -2.63 and -2.36 eV, respectively. To better understand their energy levels as films on ITO substrates, ultraviolet photoelectron spectroscopy (UPS, Figure S6, Supporting Information) was further employed to determine the HOMO levels of PPE1 and PPE2 to be -5.11 and -5.08 eV, respectively, which are consistent with those obtained from CV measurements. Overall, the suitable energy levels of both PPEs should be able to enable the hole transfer and the electron blocking when used as HTMs.

The surface wettability of polymer thin films was also evaluated as shown in Figure 3c. Both PPEs are found to have hydrophobic surface with a similar water contact angle of $\approx 90^\circ$, which could be beneficial for achieving large grain size crystals.^[24] They also have a comparable surface wettability to the polar DMF, the common solvent used for processing perovskites, with a contact angle of $\approx 20^\circ$. This suggests the feasibility of achieving good perovskite film formation with complete coverage on the PPE surface without the need of using pretreatment or surface engineering, which is important for large area blade-coating and roll-to-roll printing.^[39]

A space-charge-limited-current (SCLC) method was used to evaluate the hole mobilities of PPEs by fabricating hole-only

devices (Figure S7, Supporting Information), and both exhibit a moderate hole mobility of $\approx 2 \times 10^{-6} \text{ cm}^2 \text{ V}^{-1} \text{ s}^{-1}$ (Table 1) compared to those reported for high-performance dopant-free HTMs.^[35–38] Nonetheless, it is worth to note that the requirement for hole mobility can be relaxed somewhat for HTMs employed in the inverted PVSCs because only a very thin HTL is needed for realizing efficient hole extraction. For example, a thin fluorene-cored small molecule HTM (≈ 10 nm) with a hole mobility of $2.18 \times 10^{-6} \text{ cm}^2 \text{ V}^{-1} \text{ s}^{-1}$ was recently reported by Ding and co-workers to show a high PCE of 19.06% in inverted PVSCs without adding any dopants.^[55]

The molecular orientation of polymer films was studied by grazing incidence wide-angle X-ray scattering (GIWAXS, Figure S8, Supporting Information). As shown, the diffractions of both polymer films are oriented along an azimuthal angle of 45° with respect to the substrate. Furthermore, the extracted scattering profiles for both PPEs in the out of plane direction show two strong peaks locating at $q = 22$ and 25 nm^{-1} , respectively, suggesting the existence of two types of face-on π - π stacking patterns with very close distances of ≈ 2.85 and $\approx 2.50 \text{ \AA}$, respectively. These interesting packing behaviors are probably due to the particular crossconjugated polymer structure with large size of π -conjugated side-chains. Furthermore, we note that PPE2 film exhibits higher diffraction intensity compared to PPE1 film (Figure S8c, Supporting Information), thereby indicating an enhanced molecular crystallinity for the former, which is attributed to its unusual zigzag-type polymer chain structure.^[71,72] These results seem to be very contradictory by comparison with the hole mobility data in which PPE1 shows a slightly higher mobility than PPE2. This discrepancy thus could be due to the limitation of SCLC measurement that emphasizes vertical charge transport.

Table 2. Device parameters of PVSCs using different polymer HTMs.

HTM	V_{oc} [V]	J_{sc} [mA cm^{-2}]	FF	PCE [%]
Dopant-free PPE1	1.03 (1.02 \pm 0.02)	15.52 (15.08 \pm 0.65)	0.70 (0.69 \pm 0.02)	11.13 (9.50 \pm 1.06)
Dopant-free PPE2	1.07 (1.06 \pm 0.01)	22.84 (21.96 \pm 0.83)	0.79 (0.77 \pm 0.02)	19.33 (18.10 \pm 0.83)
Dopant-free PPE2 ^{a)}	1.18 (1.16 \pm 0.02)	22.30 (22.17 \pm 0.56)	0.81 (0.79 \pm 0.02)	21.31 (19.77 \pm 0.95)
Doped PTAA ^{a)}	1.19 (1.17 \pm 0.01)	22.65 (22.36 \pm 0.77)	0.80 (0.79 \pm 0.03)	21.56 (19.49 \pm 1.30)

^{a)} Devices treated with surface passivation by phenethylammonium iodide (PEAI).

The inverted p–i–n planar PVSCs with a configuration of ITO/HTLs/perovskite/PCBM/Ag were fabricated to study the effectiveness of **PPE1** and **PPE2** as dopant-free HTMs (**Figure 4a**). The energy-level alignments of polymer HTMs relative to perovskites are shown in **Figure 4b**, indicating that both polymers could be used for hole extraction. The HTLs were processed by spin-coating a CB solution (2 mg mL⁻¹) of polymers on ITO without adding any dopants, followed by annealing at 150 °C for 10 min. (FAPbI₃)_{0.83}(MAPbBr₃)_{0.17} (FA: formamidinium, MA: methylammonium) is used as the light-absorber, in which a small amount of NH₄BF₄ is doped to improve the device performance according to our previous work.^[73] The device fabrication details are described in the Supporting Information.

The current density–voltage (*J*–*V*) curves of the champion dopant-free inverted PVSCs measured under AM 1.5 G irradiation at 100 mW cm⁻² are shown in **Figure 4c**, with relevant device parameters summarized in **Table 2**. Interestingly, although **PPE1** and **PPE2** have a similar transparent window, HOMO energy levels and hole mobilities, they produce dramatically distinct device performance. **PPE1** only delivers a low PCE of 11.13% with a V_{oc} of 1.03 V, a short-circuit current density (J_{sc}) of 15.52 mA cm⁻², and a fill factor (FF) of 69.54%, while for **PPE2**, a significantly enhanced PCE of 19.33% is achieved with a V_{oc} of 1.07 V, a J_{sc} of 22.84 mA cm⁻², and a FF of 79.08%. The PCE histograms are provided in **Figure 4d**, showing very good reproducibility of our fabricated PVSCs with an average PCE of 9.5% for **PPE1** and 18.1% for **PPE2**, respectively.

Moreover, a stabilized PCE (18.25%) and J_{sc} (20.50 mA cm⁻²) can also be obtained for the **PPE2**-based champion device when operated at the maximum power point (0.89 V), suggesting the high reliability of the *J*–*V* curves (**Figure 4e**). The external quantum efficiency (EQE) spectra (**Figure 4f**) were also collected, and the **PPE2**-based device shows a much higher photo-response throughout the entire spectrum from 300 to 800 nm compared to that from **PPE1**-based device, confirming its much enhanced J_{sc} . Furthermore, the integrated J_{sc} value is calculated to be 14.26 mA cm⁻² for **PPE1** and 21.97 mA cm⁻² for **PPE2**, respectively, close to those of the experimental values.

Previous studies have shown that surface defect passivation is an effective strategy to boost the device performance of PVSCs.^[74] As shown, although the device based on **PPE2** can achieve a respectable PCE of 19.33%, it is still limited by its relatively low V_{oc} (1.07 V) compared to those from the state-of-the-art inverted PVSCs,^[15–19] which could be due to the misalignment between the HOMO levels of PPEs (\approx –5.1 eV) and the valence band (VB) of the perovskite (\approx –5.7 eV) as shown **Figure 4b**. Recently, Huang

and co-workers have demonstrated a very high V_{oc} of 1.23 V in inverted PVSCs by passivating the perovskite surface to suppress nonradiative recombination caused by the defects.^[19] Inspired by this work, we have also fabricated surface passivated PVSCs based on the **PPE2** HTM trying to further improve the device performance (**Figure 5a**). The PTAA-based control devices doped with 2,3,5,6-tetrafluoro-7,7,8,8-tetracyanoquinodimethane (F4-TCNQ) were also fabricated for comparison. The *J*–*V* curves of champion devices are shown in **Figure 5b**, with related data listed in **Table 2**. An organic salt phenethylammonium iodide (PEAI) was used as the surface defect passivator, according to the report by You and co-workers.^[75] The V_{oc} of PEAi passivated PVSCs is significantly improved from 1.07 to 1.18 V, without sacrificing any other device parameters, leading to a very impressive PCE of 21.31% with negligible current hysteresis (**Figure S9**, Supporting Information). This value is comparable to that from F4-TCNQ-doped PTAA based control devices (21.56%). Interestingly, we also found that **PPE2** exhibits a relatively high HOMO level compared to that of PTAA (\approx –5.2 eV), but the resulting devices show a comparable V_{oc} with each other. This might be attributed to the change of the quasi-Fermi level splitting (V_{ap}) within the perovskites grown from different HTMs.^[76,77] Furthermore, the PCE histogram of **PPE2**-based devices (**Figure 5c**) also indicates good reproducibility with an average PCE of 19.77%. It is worth noting that the device PCE of 21.31% is among the best values achieved for dopant-free HTMs, including small molecules and polymers,^[35–38] and it is very close to the record-high PCE (21.6%) reported for single-junction inverted PVSCs.^[18] Combining with their low synthetic cost and proper wettability, our results demonstrate the great potential of using crossconjugated polymer HTMs for PVSCs.

Given that PPEs are isomeric polymers with very similar optoelectronic properties, it would be interesting to understand the reason why such distinctly different device performance is obtained. To probe this, we try to investigate the effect of HTL itself by using perovskite films not passivated by PEAi. The hole extraction/transfer properties of fabricated devices were then investigated by collecting steady-state photoluminescence (PL, **Figure S10**, Supporting Information) and time-resolved PL spectra (**Figure 6a**) of the bi-layered perovskite/dopant-free HTM films. As shown, the PL of perovskites at \approx 766 nm can be completely quenched when capping with the polymer HTMs, while the average PL decay time (τ) of bilayered films are also significantly shortened relative to that of bare perovskite film (\approx 1324 ns, **Table S5**, Supporting Information). Both indicate an efficient extraction of holes from the perovskite without the need of using any dopants. However, the τ for **PPE1** (24 ns) is found to be much

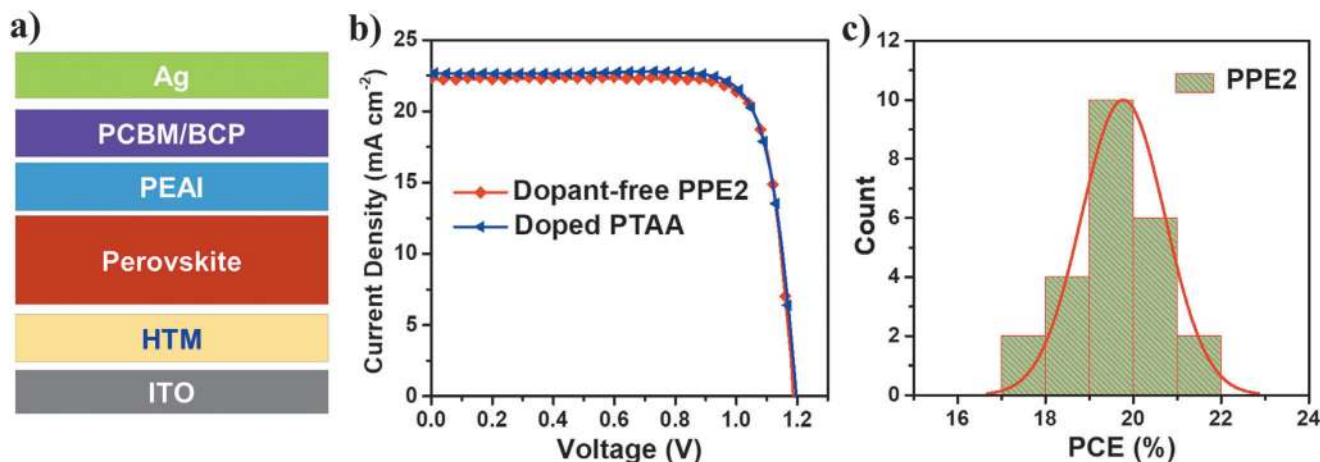


Figure 5. a) Device structure containing surface passivation layer of PEAI; b) J - V curves of the champion PVSCs based on dopant-free PPE2 and doped PTAA HTMs; c) histograms of efficiency distributions of fabricated PVSCs based on dopant-free PPE2 HTM.

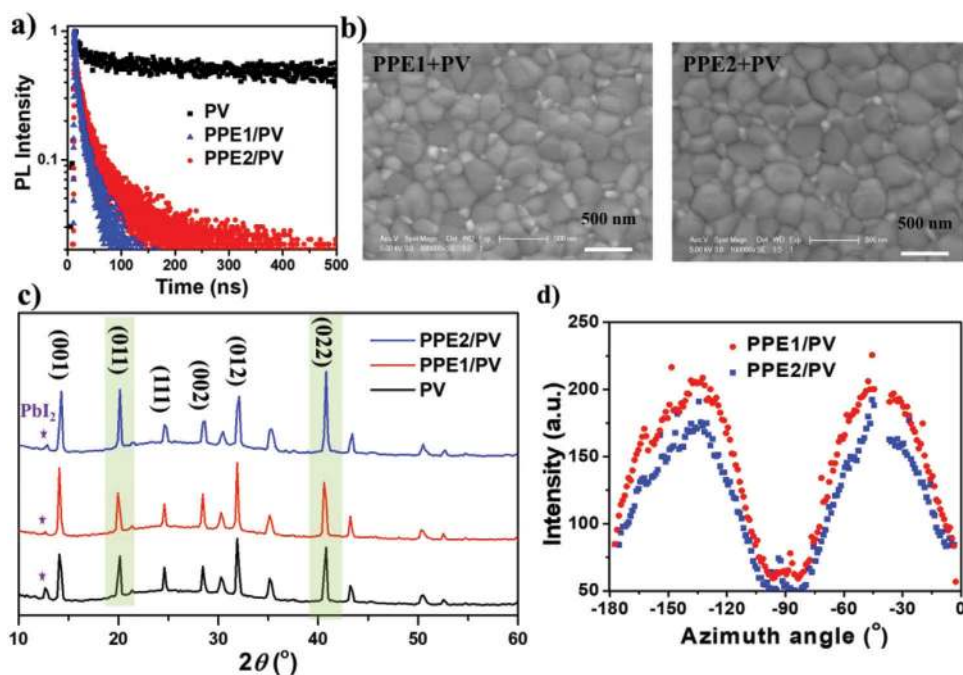


Figure 6. a) Time-resolved PL spectra of bare perovskite (PV) film and bilayered PV films capped with dopant-free polymer HTMs; b) SEM images of PV films atop PPEs; c) XRD patterns of bare PV film and bilayered PV films atop PPEs; d) The azimuthal intensity distributions for (100) plane in GIWAXS patterns of PV films atop PPEs. Note that the PV films were not passivated.

shorter than that for PPE2 (42 ns), while the PPE2-based devices show much higher PCEs reversely. The common experience tells us faster decay time usually indicates more efficient hole extraction/transport and better suppressed charge recombination, which will result in higher device performance.^[78–83] Therefore, there must be some other underlying factors related to the quality of perovskite film causing these controversial results. Indeed, for inverted PVSCs, the HTM morphology has been shown to play an important role in determining the growth of perovskite and its final film quality on top including grain sizes, crystal orientation, and defects.^[27,28] Furthermore, the time-resolved PL spectrum of

the PPE2-based passivated film was also measured, as shown in Figure S11 (Supporting Information) the τ greatly increases from 42 to 70 ns due to the PEAI passivation, further indicating the surface passivation of defects can effectively suppress the non-radiation recombination.

The surface morphology of the perovskite films was then investigated through the plane-view scanning electron microscope (SEM, Figure 6b). It was found that the perovskite film atop of PPE2 obviously exhibits larger grain sizes than that atop of PPE1. The crystallinity of perovskite films was further checked by studying their X-ray powder diffraction (XRD) patterns. As shown in

Figure 6c, all the characteristic crystallographic planes of perovskite can be observed, and the peak intensity of PbI_2 is significantly decreased for perovskites made atop of polymer HTMs, meaning enhanced film quality. The residual signal of PbI_2 in perovskite films on PPEs is attributed to the use of slightly excess PbI_2 in preparing the perovskite films to reduce the defects.^[84] Encouragingly, the relative diffraction intensities of (011) and (022) crystallographic planes (Figure S12, Supporting Information) are much higher for perovskite film atop **PPE2**, comparing with those from **PPE1**. These results suggest a better quality of perovskite films produced atop of **PPE2**.

To assess the cause of different crystallinities in perovskite films, GIWAXS measurements were further conducted. As shown in Figure S13 (Supporting Information), the (100) and (200) crystal planes of resulting perovskites showed a q of 10 and 21 nm^{-1} , respectively, indicating a preferred orientation along the azimuthal angle of 43° with respect to the substrate, similar to the reported results.^[85] In addition, both planes of perovskite films atop of **PPE2** show narrower azimuthal intensity distributions than those from **PPE1** (Figures 6d and Figure S14, Supporting Information), strongly suggesting a better oriented crystals for the former. Based on these results, it is reasonable to conclude that the significantly improved PCE for **PPE2** derived devices is due to its ability in enabling better quality perovskite films with more oriented crystals. This results in reduced charge traps and carrier recombination,^[86] thereby explains why the perovskite film atop of **PPE2** has a longer decay time than **PPE1**. Since both PPEs exhibit similar structure and properties, the most likely reason for the significant PCE difference could be due to the enhanced molecular crystallinity of **PPE2** in solid films as discussed above, enabling it as a potential template to facilitate the growth of ordered perovskite films with enhanced crystallinity through the van der Waals interactions between perovskite and HTL.^[22,27,28]

3. Conclusion

In conclusion, we have developed a simple and effective way to synthesize two novel crossconjugated *iso*-PTAs, **PPE1** and **PPE2**, by changing the linking positions of phenyl spacers from para to meta, in which 2,7-diphenylamine capped fluorene units are attached to the vinylidene groups as side-chains. By using these polymers as dopant-free HTMs in inverted PVSCs, dramatically distinct PCEs of 11.13% for **PPE1** with paraconjugation and 19.33% for **PPE2** with metaconjugation were obtained. Through further application of PEAI to passivate the defects of perovskites, the V_{oc} of **PPE2**-derived device was significantly improved from 1.07 to 1.18 V, affording a very impressive PCE of 21.31%. Given the fact that **PPE1** and **PPE2** are isomeric polymers with similar optical properties, surface wettability, energy levels, and hole mobilities, the significantly enhanced device performance of **PPE2**-based PVSCs could be attributed to the enhanced perovskite quality grown atop its film. **PPE2** might serve as a good template to facilitate the growth of perovskites with larger grain sizes and more oriented crystals. This work provides a simple and effective way in developing high-performance dopant-free HTMs and highlights the critical role of HTL in affecting the perovskite growth/crystallization in inverted PVSCs.

Supporting Information

Supporting Information is available from the Wiley Online Library or from the author.

Acknowledgements

X.S. and X.D. contributed equally to this work. Z.L. thanks the financial support from the National Natural Science Foundation of China (Nos. 21704030 and 21975085). C.Z. thanks the financial support from the National Science Foundation of China (No. 51873160). Z.Z. and A.J. thank the New Faculty Start-up Grant of the City University of Hong Kong (Nos. 9610421 and 7200587).

Conflict of Interest

The authors declare no conflict of interest.

Keywords

crossconjugated polymers, dopant-free hole-transporting materials, perovskite growth, perovskite solar cells

Received: November 21, 2019
Revised: March 6, 2020
Published online: May 28, 2020

- [1] A. Kojima, K. Teshima, Y. Shirai, T. Miyasaka, *J. Am. Chem. Soc.* **2009**, *131*, 6050.
- [2] Chart listing the best photovoltaic cell efficiencies, provided by NREL, <https://www.nrel.gov/pv/assets/images/efficiency-chart.png> (accessed: November 2019).
- [3] M. A. Green, A. Ho-Baillie, H. J. Snaith, *Nat. Photonics* **2014**, *8*, 506.
- [4] P. K. Nayak, S. Mahesh, H. J. Snaith, D. Cahen, *Nat. Rev. Mater.* **2019**, *4*, 269.
- [5] A. Rajagopal, K. Yao, A. K.-Y. Jen, *Adv. Mater.* **2018**, *30*, 1800455.
- [6] A. K. Jena, A. Kulkarni, T. Miyasaka, *Chem. Rev.* **2019**, *119*, 3036.
- [7] H. S. Jung, N. G. Park, *Small* **2015**, *11*, 10.
- [8] L. Meng, J. You, T.-F. Guo, Y. Yang, *Acc. Chem. Res.* **2016**, *49*, 155.
- [9] Y. Rong, Y. Hu, A. Mei, H. Tan, M. I. Saidaminov, S. I. Seok, M. D. McGehee, E. H. Sargent, H. Han, *Science* **2018**, *361*, eaat8235.
- [10] P. Docampo, J. M. Ball, M. Darwich, G. E. Eperon, H. J. Snaith, *Nat. Commun.* **2013**, *4*, 2761.
- [11] T. Liu, K. Chen, Q. Hu, R. Zhu, Q. Gong, *Adv. Energy Mater.* **2016**, *6*, 1600457.
- [12] Y. Bai, X. Meng, S. Yang, *Adv. Energy Mater.* **2018**, *8*, 1701883.
- [13] C. Zuo, H. J. Bolink, H. Han, J. Huang, D. Cahen, L. Ding, *Adv. Sci.* **2016**, *3*, 1500324.
- [14] J.-Y. Jeng, Y.-F. Chiang, M.-H. Lee, S.-R. Peng, T.-F. Guo, P. Chen, T.-C. Wen, *Adv. Mater.* **2013**, *25*, 3727.
- [15] S. Yue, K. Liu, R. Xu, M. Li, M. Azam, K. Ren, J. Liu, Y. Sun, Z. Wang, D. Cao, X. Yan, S. Qu, Y. Lei, Z. Wang, *Energy Environ. Sci.* **2017**, *10*, 2570.
- [16] K. Yao, S. Leng, Z. Liu, L. Fei, Y. Chen, S. Li, N. Zhou, J. Zhang, Y.-X. Xu, L. Zhou, H. Huang, A. K. Y. Jen, *Joule* **2019**, *3*, 417.
- [17] D. Luo, W. Yang, Z. Wang, A. Sadhanala, Q. Hu, R. Su, R. Shivanna, G. F. Trindade, J. F. Watts, Z. Xu, T. Liu, K. Chen, F. Ye, P. Wu, L. Zhao, J. Wu, Y. Tu, Y. Zhang, X. Yang, W. Zhang, R. H. Friend, Q. Gong, H. J. Snaith, R. Zhu, *Science* **2018**, *360*, 1442.

- [18] M. Stolterfoht, C. M. Wolff, J. A. Márquez, S. Zhang, C. J. Hages, D. Rothhardt, S. Albrecht, P. L. Burn, P. Meredith, T. Unold, D. Neher, *Nat. Energy* **2018**, *3*, 847.
- [19] S. Yang, J. Dai, Z. Yu, Y. Shao, Y. Zhou, X. Xiao, X. C. Zeng, J. Huang, *J. Am. Chem. Soc.* **2019**, *141*, 5781.
- [20] B. Li, C. Zheng, H. Liu, J. Zhu, H. Zhang, D. Gao, W. Huang, *ACS Appl. Mater. Interfaces* **2016**, *8*, 27438.
- [21] F. Galatopoulos, A. Savva, I. T. Papadas, S. A. Choulis, *APL Mater.* **2017**, *5*, 076102.
- [22] G. Tang, P. You, Q. Tai, A. Yang, J. Cao, F. Zheng, Z. Zhou, J. Zhao, P. K. L. Chan, F. Yan, *Adv. Mater.* **2019**, *31*, 1807689.
- [23] C. Liu, J. Tu, X. Hu, Z. Huang, X. Meng, J. Yang, X. Duan, L. Tan, Z. Li, Y. Chen, *Adv. Funct. Mater.* **2019**, *29*, 1808059.
- [24] C. Bi, Q. Wang, Y. Shao, Y. Yuan, Z. Xiao, J. Huang, *Nat. Commun.* **2015**, *6*, 7747.
- [25] J. Lee, H. Kang, G. Kim, H. Back, J. Kim, S. Hong, B. Park, E. Lee, K. Lee, *Adv. Mater.* **2017**, *29*, 1606363.
- [26] Q. Xiao, F. Wu, M. Han, Z. Li, L. Zhu, Z. Li, *J. Mater. Chem. A* **2018**, *6*, 13644.
- [27] Z.-K. Wang, X. Gong, M. Li, Y. Hu, J.-M. Wang, H. Ma, L.-S. Liao, *ACS Nano* **2016**, *10*, 5479.
- [28] X. Zhao, L. Tao, H. Li, W. Huang, P. Sun, J. Liu, S. Liu, Q. Sun, Z. Cui, L. Sun, Y. Shen, Y. Yang, M. Wang, *Nano Lett.* **2018**, *18*, 2442.
- [29] Q. Xue, G. Chen, M. Liu, J. Xiao, Z. Chen, Z. Hu, X.-F. Jiang, B. Zhang, F. Huang, W. Yang, H.-L. Yip, Y. Cao, *Adv. Energy Mater.* **2016**, *6*, 1502021.
- [30] K.-G. Lim, S. Ahn, Y.-H. Kim, Y. Qi, T.-W. Lee, *Energy Environ. Sci.* **2016**, *9*, 932.
- [31] W. Yan, S. Ye, Y. Li, W. Sun, H. Rao, Z. Liu, Z. Bian, C. Huang, *Adv. Energy Mater.* **2016**, *6*, 1600474.
- [32] W. S. Yang, B.-W. Park, E. H. Jung, N. J. Jeon, Y. C. Kim, D. U. Lee, S. S. Shin, J. Seo, E. K. Kim, J. H. Noh, S. I. Seok, *Science* **2017**, *356*, 1376.
- [33] Q. Wang, C. Bi, J. Huang, *Nano Energy* **2015**, *15*, 275.
- [34] C.-I. Chen, S. Wu, Y.-A. Lu, C.-C. Lee, K.-C. Ho, Z. Zhu, W.-C. Chen, C.-C. Chueh, *Adv. Sci.* **2019**, *6*, 1901714.
- [35] W. Zhou, Z. Wen, P. Gao, *Adv. Energy Mater.* **2018**, *8*, 1702512.
- [36] X. Sun, D. Zhao, Z. Li, *Chin. Chem. Lett.* **2018**, *29*, 219.
- [37] K. Rakstys, C. Igci, M. K. Nazeeruddin, *Chem. Sci.* **2019**, *10*, 6748.
- [38] H. D. Pham, X. Li, W. Li, S. Manzhos, A. K. K. Kyaw, P. Sonar, *Energy Environ. Sci.* **2019**, *12*, 1177.
- [39] W.-Q. Wu, Q. Wang, Y. Fang, Y. Shao, S. Tang, Y. Deng, H. Lu, Y. Liu, T. Li, Z. Yang, A. Gruverman, J. Huang, *Nat. Commun.* **2018**, *9*, 1625.
- [40] W. Zhang, Y.-C. Wang, X. Li, C. Song, L. Wan, K. Usman, J. Fang, *Adv. Sci.* **2018**, *5*, 1800159.
- [41] C.-H. Tsai, N. Li, C.-C. Lee, H.-C. Wu, Z. Zhu, L. Wang, W.-C. Chen, H. Yan, C.-C. Chueh, *J. Mater. Chem. A* **2018**, *6*, 12999.
- [42] D. Yang, T. Sano, Y. Yaguchi, H. Sun, H. Sasabe, J. Kido, *Adv. Funct. Mater.* **2019**, *29*, 1807556.
- [43] L. Zhang, X. Zhou, X. Zhong, C. Cheng, Y. Tian, B. Xu, *Nano Energy* **2019**, *57*, 248.
- [44] M. Gholami, R. R. Tykwinski, *Chem. Rev.* **2006**, *106*, 4997.
- [45] T. P. Voortman, D. Bartesaghi, L. J. A. Koster, R. C. Chiechi, *Macromolecules* **2015**, *48*, 7007.
- [46] Y. Yao, H. Dong, F. Liu, T. P. Russell, W. Hu, *Adv. Mater.* **2017**, *29*, 1701251.
- [47] Y. Zhang, H. Cheema, A. E. London, A. Morales, J. D. Azoulay, J. H. Delcamp, *Phys. Chem. Chem. Phys.* **2018**, *20*, 2438.
- [48] W. Zhang, Z. Mao, N. Zheng, J. Zou, L. Wang, C. Wei, J. Huang, D. Gao, G. Yu, *J. Mater. Chem. C* **2016**, *4*, 9266.
- [49] G. W. P. Pruijsen, J. Brebels, K. H. Hendriks, M. M. Wienk, R. A. J. Janssen, *Macromolecules* **2015**, *48*, 2435.
- [50] Y. Zhao, R. R. Tykwinski, *J. Am. Chem. Soc.* **1999**, *121*, 458.
- [51] Y. Zhao, R. McDonald, R. R. Tykwinski, *J. Org. Chem.* **2002**, *67*, 2805.
- [52] M. M. Rahman, X. Zhao, J. Harrell, L. Chen, A. Pietrangelo, *ACS Macro Lett.* **2017**, *6*, 632.
- [53] S. C. Ciulei, R. R. Tykwinski, *J. Org. Chem.* **2000**, *2*, 3607.
- [54] Y. Zhao, R. McDonald, R. R. Tykwinski, *Chem. Commun.* **2000**, 77.
- [55] J. Zhang, Q. Sun, Q. Chen, Y. Wang, Y. Zhou, B. Song, N. Yuan, J. Ding, Y. Li, *Adv. Funct. Mater.* **2019**, *29*, 1900484.
- [56] H. D. Pham, L. Gil-Escrig, K. Feron, S. Manzhos, S. Albrecht, H. J. Bolink, P. Sonar, *J. Mater. Chem. A* **2019**, *7*, 12507.
- [57] Y. Zhang, C. Kou, J. Zhang, Y. Liu, W. Li, Z. Bo, M. Shao, *J. Mater. Chem. A* **2019**, *7*, 5522.
- [58] J. Zhang, B. Xu, L. Yang, A. Mingorance, C. Ruan, Y. Hua, L. Wang, N. Vlachopoulos, M. Lira-Cantú, G. Boschloo, A. Hagfeldt, L. Sun, E. M. J. Johansson, *Adv. Energy Mater.* **2017**, *7*, 1602736.
- [59] H.-C. Liao, T. L. D. Tam, P. Guo, Y. Wu, E. F. Manley, W. Huang, N. Zhou, C. M. M. Soe, B. Wang, M. R. Wasielewski, L. X. Chen, M. G. Kanatzidis, A. Facchetti, R. P. H. Chang, T. J. Marks, *Adv. Energy Mater.* **2016**, *6*, 1600502.
- [60] G.-W. Kim, G. Kang, J. Kim, G.-Y. Lee, H. I. Kim, L. Pyeon, J. Lee, T. Park, *Energy Environ. Sci.* **2016**, *9*, 2326.
- [61] K. Kranthiraja, K. Gunasekar, H. Kim, A. N. Cho, N. G. Park, S. Kim, B. J. Kim, R. Nishikubo, A. Saeki, M. Song, S. H. Jin, *Adv. Mater.* **2017**, *29*, 1700183.
- [62] G.-W. Kim, J. Lee, G. Kang, T. Kim, T. Park, *Adv. Energy Mater.* **2018**, *8*, 1701935.
- [63] J. Lee, M. M. Byranvand, G. Kang, S. Y. Son, S. Song, G. W. Kim, T. Park, *J. Am. Chem. Soc.* **2017**, *139*, 12175.
- [64] F. Qi, X. Deng, X. Wu, L. Huo, Y. Xiao, X. Lu, Z. Zhu, A. K. Y. Jen, *Adv. Energy Mater.* **2019**, *9*, 1902600.
- [65] G. You, Q. Zhuang, L. Wang, X. Lin, D. Zou, Z. Lin, H. Zhen, W. Zhuang, Q. Ling, *Adv. Energy Mater.* **2020**, *10*, 1903146.
- [66] Q. Xiao, J. Tian, Q. Xue, J. Wang, B. Xiong, M. Han, Z. Li, Z. Zhu, H.-L. Yip, Z. a. Li, *Angew. Chem., Int. Ed.* **2019**, *58*, 17724.
- [67] X. Sun, Q. Xue, Z. Zhu, Q. Xiao, K. Jiang, H. L. Yip, H. Yan, Z. Li, *Chem. Sci.* **2018**, *9*, 2698.
- [68] Z.-Q. Chen, T. Chen, J.-X. Liu, G.-F. Zhang, C. Li, W.-L. Gong, Z.-J. Xiong, N.-H. Xie, B. Z. Tang, M.-Q. Zhu, *Macromolecules* **2015**, *48*, 7823.
- [69] C. Huang, W. Fu, C. Z. Li, Z. Zhang, W. Qiu, M. Shi, P. Heremans, A. K. Jen, H. Chen, *J. Am. Chem. Soc.* **2016**, *138*, 2528.
- [70] S. Ahmad, P. K. Kanaujia, W. Niu, J. J. Baumberg, G. Vijaya Prakash, *ACS Appl. Mater. Interfaces* **2014**, *6*, 10238.
- [71] I. Osaka, T. Abe, S. Shinamura, E. Miyazaki, K. Takimiya, *J. Am. Chem. Soc.* **2010**, *132*, 5000.
- [72] S. Shi, X. Xie, P. Jiang, S. Chen, L. Wang, M. Wang, H. Wang, X. Li, G. Yu, Y. Li, *Macromolecules* **2013**, *46*, 3358.
- [73] J. Zhang, S. Wu, T. Liu, Z. Zhu, A. K.-Y. Jen, *Adv. Funct. Mater.* **2019**, *29*, 1808833.
- [74] E. Aydin, M. De Bastiani, S. De Wolf, *Adv. Mater.* **2019**, *31*, 1900428.
- [75] Q. Jiang, Y. Zhao, X. Zhang, X. Yang, Y. Chen, Z. Chu, Q. Ye, X. Li, Z. Yin, J. You, *Nat. Photonics* **2019**, *13*, 460.
- [76] R. A. Belisle, P. Jain, R. Prasanna, T. Leijtens, M. D. McGehee, *ACS Energy Lett.* **2016**, *1*, 556.
- [77] M. Stolterfoht, P. Caprioglio, C. M. Wolff, J. A. Márquez, J. Nordmann, S. Zhang, D. Rothhardt, U. Hörmann, Y. Amir, A. Redinger, L. Kegelmann, F. Zu, S. Albrecht, N. Koch, T. Kirchartz, M. Saliba, T. Unold, D. Neher, *Energy Environ. Sci.* **2019**, *12*, 2778.
- [78] C. Shen, Y. Wu, H. Zhang, E. Li, W. Zhang, X. Xu, W. Wu, H. Tian, W.-H. Zhu, *Angew. Chem., Int. Ed.* **2019**, *58*, 3784.
- [79] S. Paek, P. Qin, Y. Lee, K. T. Cho, P. Gao, G. Grancini, E. Oveisi, P. Gratia, K. Rakstys, S. A. Al-Muhtaseb, C. Ludwig, J. Ko, M. K. Nazeeruddin, *Adv. Mater.* **2017**, *29*, 1606555.

- [80] F. Liu, F. Wu, Z. Tu, Q. Liao, Y. Gong, L. Zhu, Q. Li, Z. Li, *Adv. Funct. Mater.* **2019**, 29, 1901296.
- [81] Y. Wang, W. Chen, L. Wang, B. Tu, T. Chen, B. Liu, K. Yang, C. W. Koh, X. Zhang, H. Sun, G. Chen, X. Feng, H. Y. Woo, A. B. Djurišić, Z. He, X. Guo, *Adv. Mater.* **2019**, 31, 1902781.
- [82] X. Sun, F. Wu, C. Zhong, L. Zhu, Z. a. Li, *Chem. Sci.* **2019**, 10, 6899.
- [83] X. Lai, F. Meng, Q.-Q. Zhang, K. Wang, G. Li, Y. Wen, H. Ma, W. Li, X. Li, A. K. K. Kyaw, K. Wang, X. W. Sun, M. Du, X. Guo, J. Wang, W. Huang, *Sol. RRL* **2019**, 3, 1900011.
- [84] B.-w. Park, N. Kedem, M. Kulbak, D. Y. Lee, W. S. Yang, N. J. Jeon, J. Seo, G. Kim, K. J. Kim, T. J. Shin, G. Hodes, D. Cahen, S. I. Seok, *Nat. Commun.* **2018**, 9, 3301.
- [85] L. Meng, C. Sun, R. Wang, W. Huang, Z. Zhao, P. Sun, T. Huang, J. Xue, J. W. Lee, C. Zhu, Y. Huang, Y. Li, Y. Yang, *J. Am. Chem. Soc.* **2018**, 140, 17255.
- [86] Z. Xu, Z. Liu, N. Li, G. Tang, G. Zheng, C. Zhu, Y. Chen, L. Wang, Y. Huang, L. Li, N. Zhou, J. Hong, Q. Chen, H. Zhou, *Adv. Mater.* **2019**, 31, 1900390.